Investigation of Self-Heating Phenomenon in Small Geometry Vias Using Scanning Joule Expansion Microscopy

Kaustav Banerjee[1*], Guanghua Wu[2], Masanobu Igeta[2**], Ajith Amerasekera[3], Arun Majumdar[2], and Chenming Hu[1]

[1]Department of Electrical Engineering and Computer Sciences, [2]Department of Mechanical Engineering, University of California, Berkeley, CA 94720

[3]Silicon Technology Development Center, Texas Instruments Inc., Dallas, TX 75243

ABSTRACT

This paper reports the use of a novel thermometry technique, scanning Joule expansion microscopy (SJEM), to study the steady state and dynamic thermal behavior of small geometry vias under sinusoidal and pulsed current stress for the first time. Spatial distribution of temperature rise surrounding a sub-micron via has been determined and the corresponding temperature contour image has been extracted. The thermal time constant of the via structure has been determined from the measured AC frequency dependence of the temperature rise. Furthermore, the average (DC) and peak temperature rise under pulsed stress condition has been estimated from the measured first harmonic temperature rise.

INTRODUCTION

The continuous scaling of VLSI circuits has resulted in an increase in the aspect ratio of the vias (connection between adjacent metallization levels) and increases in the current density and associated thermal effects, namely self-heating. Current crowding and localized heating [1], [2], [3] in deep sub-micrometer vias are known to strongly impact reliability of VLSI interconnects. The magnitude and spatial distribution of the temperature rise in the via are important to accurately estimate interconnect lifetime under electromigration (EM), which is temperature dependent. Localized temperature rise can also cause stress gradients inside the via structures and can also lead to melting under short-duration high current stress conditions, such as electrostatic discharge (ESD) events [4]. Hence, measurements of the magnitude and spatial distribution of the temperature rise in deep sub-micrometer vias are important to accurately model their reliability and provide thermal design guidelines for various via technologies.

In general, interconnect thermometry based on temperature-dependent electrical resistivity of the interconnect metal is used to calculate a spatially averaged temperature rise along the interconnects [5]. However, this does not provide local temperature rise which may be much higher around vias. The spatial resolution of far-field optical techniques, such as scanning thermoreflectance thermometry [6], infrared thermography [7], and liquid crystal thermography [8], is diffraction-limited to about 1 μm. This is insufficient to probe deep sub-micrometer vias in the size range of 0.1-0.5 μm. Near-field optics can be employed to overcome the diffraction limit [9], but it is still in its infancy as far as accurate measurements of all desired parameters are concerned. The SJEM, has recently been developed with spatial resolution in the sub-0.1 μm range [10]. In this work, SJEM is used to study the thermal characteristics of small geometry W-plug vias.

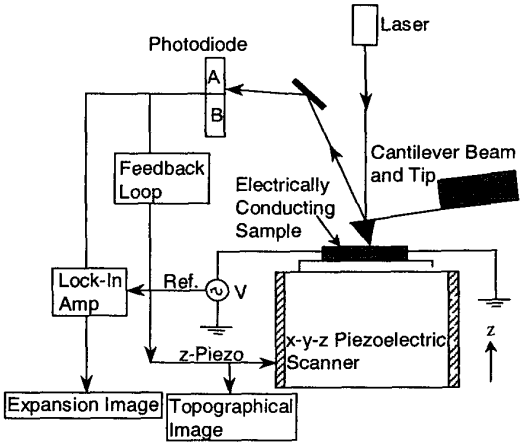

Fig. 1. Schematic diagram of the experimental setup used for the scanning Joule expansion microscopy (SJEM).

SJEM SYSTEM DESIGN

Figure 1 shows the schematic diagram of the scanning Joule expansion microscope (SJEM) system used in this study. An atomic force microscope (AFM) is used to bring a sharp tip into force-controlled contact with the sample surface and perform a raster scan. A sinusoidal or pulsed voltage is applied to the electrically conducting sample (W-Via) which produces sample Joule heating and temperature rise, resulting in sample thermal expansion. A low-power laser beam incident on the AFM tip changes its location on the photodiode due to deflection of the tip. The location of the laser beam on the photodiode determines the output signal of the photodiode. The AFM photodiode detects the cantilever deflection due to both expansion and sample topography. Since the feedback controller of the AFM has a bandwidth of 5 KHz, the photodiode signal below 5 KHz is processed for feedback control of the z-piezo to image surface topography under constant tip-sample force or cantilever deflection. The Joule heating frequency is kept above 5 KHz to avoid feedback response. The lock-in amplifier is tuned to the Joule heating frequency, which detects only the expansion signal and provides this to an auxiliary AFM channel to form the expansion image. The system can also be operated without feedback in which case the heating frequency can be below the controller bandwidth [10], [11].

* Now with the Center for Integrated Systems, Department of Electrical Engineering, Stanford University, Stanford, CA 94305.

** Visiting Student from the Department of Mechano-Aerospace Engineering, Tokyo Institute of Technology, Tokyo 152, Japan.

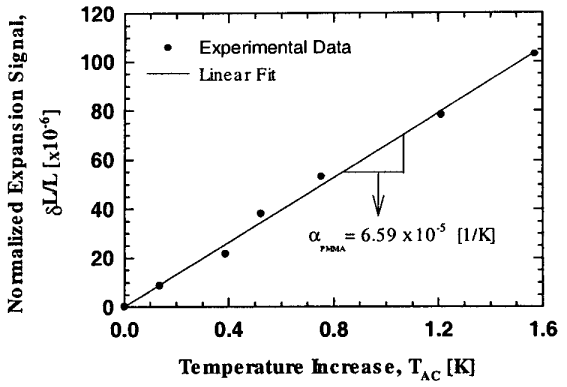

Fig. 2. The thermal expansion coefficient of PMMA determined by measuring the expansion signal and calculating the corresponding AC temperature rise of an Al-Cu line from the measured amplitude of the 3ω component of the voltage signal using the lock-in amplifier.

SAMPLE FABRICATION

The W-plug via structures were fabricated in a state-of-the-art 0.25 μm industrial CMOS process flow. The samples used in the experiments contained 0.6 μm-thick Al-Cu interconnects (with top and bottom layers of 0.05 and 0.1 μm-thick TiN) at two levels of metallization that were separated by a layer of ~0.9 μm-thick silicon dioxide. These interconnects crossed each other forming an overlapping region and were bridged in this region by a single W-plug via with 0.4 μm diameter. Both levels of AlCu lines were 1.6 μm wide. The samples were coated with a standard passivation layer of ~1.0 μm thick silicon dioxide followed by a capping layer of 0.3 μm thick silicon nitride. Since the thermal expansion coefficient of the oxide and nitride is low, a 0.28 μm thick film of polymethyl methacrylate (PMMA) was spin coated on the sample to amplify the expansion signal. PMMA film can be easily striped off using acetone after all the measurements. This procedure is feasible for routine investigations since it is easy and safe to be accomplished. The thermal expansion coefficient of PMMA is typically about 7×10^{-5} K^{-1}, which results in a sensitivity of 2.0×10^{-11} m/K and a temperature resolution of about 0.2 K.

TEMPERATURE CALIBRATION

Since the expansion signal of the PMMA film dominated over other layers on the sample, it was necessary to accurately determine the expansion coefficient of the PMMA film in order to convert expansion signals to temperature rise. This was achieved by first measuring the electrical resistance of an AlCu interconnect as a function of temperature and extracting the temperature coefficient of resistance (β) of AlCu. The expansion signal of the PMMA film over the AlCu interconnect was then measured using an AC bias current given by,

$$I = I_0 \cos \omega t \qquad (1)$$

The resistance of the AlCu line under such bias is given by,

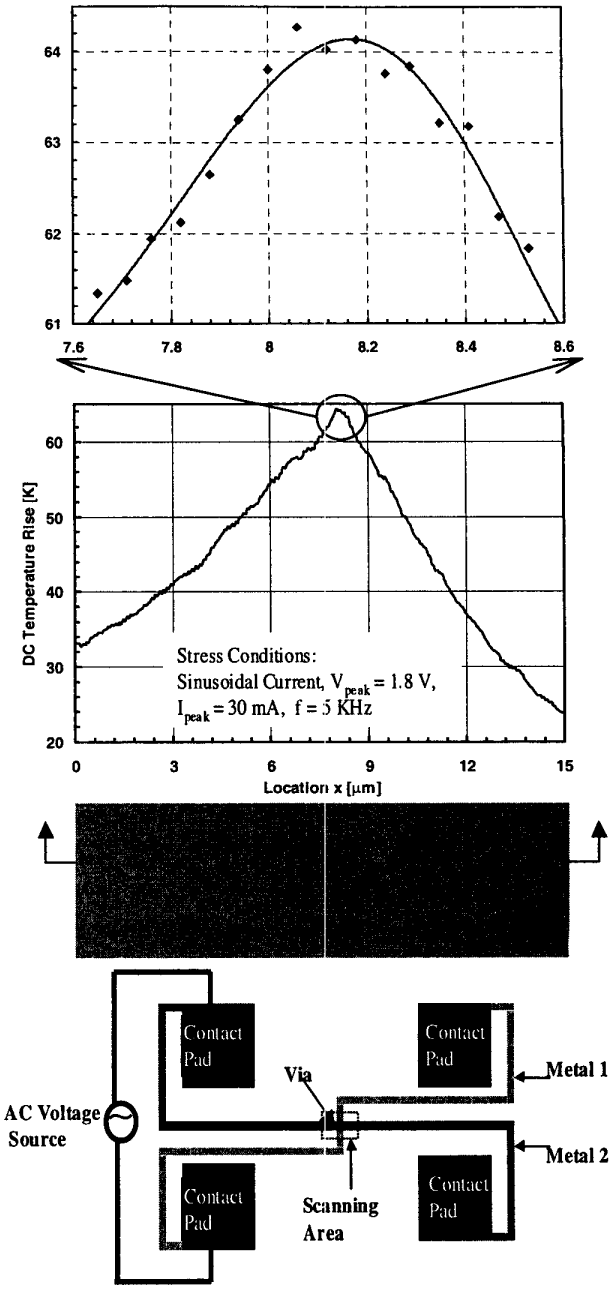

Fig. 3. Temperature profile and the temperature contour image of the 0.4 μm via sample measured by SJEM. Also shown is the top-view of the via sample. The dashed-line box indicates the scanning area of the AFM cantilever.

$$R = R_0 \{1 + \beta (T_{DC} + T_{AC} \cos(2\omega t + \varphi))\} \qquad (2)$$

Where T_{DC} and T_{AC} are the DC and peak AC temperature rises respectively. ϕ is the phase lag between the current and the temperature and ω (=$2\pi f$) is the angular frequency. Therefore, the voltage across the line is given by,

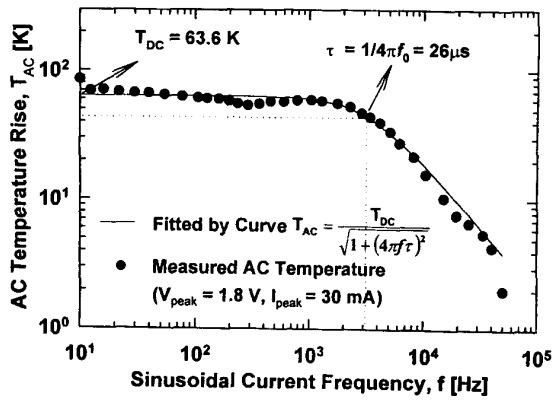

Fig. 4. Experimental data showing extraction of a time constant τ = 26 μs for the via structure. Note that τ is a characteristic of the thermal system and is independent of the waveform.

$$V = I_0 R_0 \left[\left\{ (1+\beta T_{DC})\cos\omega t + \frac{\beta T_{AC}}{2}\cos(\omega t+\varphi) \right\} + \frac{\beta T_{AC}}{2}\cos(3\omega t+\varphi) \right] \quad (3)$$

The lock-in amplifier locks in to the 3ω component of the voltage and measures the amplitude ($\frac{I_0 R_0 \beta T_{AC}}{2}$) of the 3ω component. We can therefore calculate T_{AC} from the measured amplitude of the 3ω component of the voltage signal.

The locally measured 2ω component of the expansion signal of the PMMA film, δL, can be expressed as,

$$\delta L = \alpha \cdot L \cdot T_{AC} \quad (4)$$

Where α is the expansion coefficient of the PMMA film, L is the PMMA film thickness. The thermal expansion coefficient of PMMA can then be experimentally obtained from equation (4) and was found to be 65.9 ± 3.3 x 10^{-6} K^{-1}as illustrated in Fig. 2. Once α has been calibrated locally, T_{AC} can be calculated directly from the measured expansion signal using equation (4).

EXPERIMENTAL RESULTS and DISCUSSIONS

Figure 3 (top) shows the spatial temperature profile of the via sample using SJEM. The temperature contour image (center) shows the hot region on top of the via. Although the vias were 0.4 μm in diameter, diffusion in the passivation layers spread the temperature peak to about 10 μm at full-width half-maximum. It must be noted that despite this lateral spread, the temperature drop across the thickness of the passivation layer and the PMMA film can be expected to be quite small. This is because the temperature rise exponentially decays from the heat source with the decay length given by $\sqrt{\kappa/\pi f}$, where κ is the thermal diffusivity of the material and f is the applied frequency [11]. The thermal diffusivity of PMMA is the lowest of the three passivation materials, and is ~10^{-7} m^2/s. Hence, if the modulation frequencies are kept below 50 KHz, the penetration depth should be larger

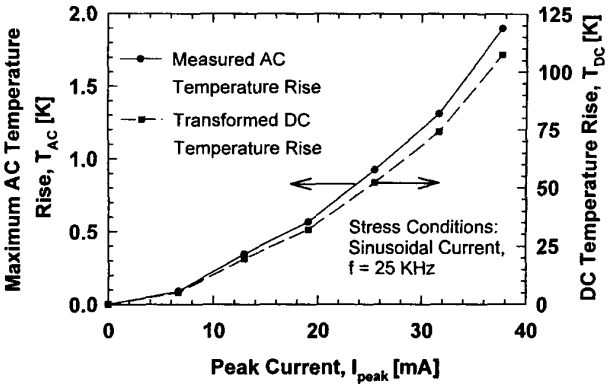

Fig. 5. The maximum AC temperature rise and the corresponding DC temperature rise under different sinusoidal current stress. The time to get one data point typically is around 15 minutes. The DC temperature rise was estimated from AC temperature rise using equation (14) and the analysis is described in the text.

than 0.8 μm, which is much larger than the PMMA film thickness (0.28 μm).

Self-Heating Analysis under Sinusoidal Bias

In addition to an AC temperature rise under a sinusoidal bias, there is also a DC temperature rise due to the value of RMS power dissipation. The DC temperature rise is often much higher than the AC component and is, therefore, of interest. Since SJEM measures only the AC component, estimation of the DC component requires analysis. The thermal behavior follows a first-order system and is characterized by a time constant τ. The governing heat equation is given by

$$mc\frac{\partial T}{\partial t} = -(h_c A)(T - T_0) + I^2 R \quad (5)$$

Where m is the sample mass, c is specific heat, R is the resistance of sample, h_c is the effective heat transfer coefficient averaged over the via surface area A. The first term on the right hand side of equation (5) represents an effective heat dissipation term under the assumption that there are no temperature gradients within the sample (Via). The validity of this assumption is based on the fact that the Biot number, Bi is < 0.1. Bi is defined as [13]

$$Bi = \frac{Internal - conduction - resis\,tan\,ce}{External - heat - transfer - resis\,tan\,ce} = \frac{L/k_s A}{1/h_c A} = \frac{h_c L}{k_s} \quad (6)$$

Where L is the characteristic length of the solid sample (W-Via), and k_s is the thermal conductivity of sample material (W). Now under an AC bias the current is given by equation (1). Substituting this expression for current in equation (5) we get,

$$mc\frac{\partial \theta}{\partial t} = -h_c A\theta + \frac{I_0^2 R}{2}[1+\cos 2\omega t] \quad (7)$$

Where $\theta = T - T_0$, the dependence of R on θ has been neglected since $R = R_0(1+\beta\theta)$ and $\beta\theta << 1$. Equation (7) can be rewritten as,

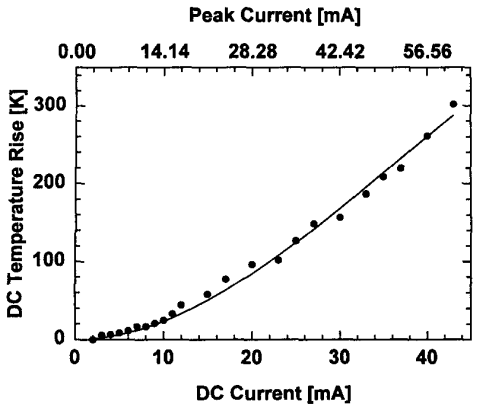

Fig. 6. Average temperature rise of the via sample determined using resistive thermometry. The corresponding peak current values for the sinusoidal bias is also shown along the second x-axis based on $I_{peak} = \sqrt{2}\, I_{DC}$.

$$\frac{\partial \theta}{\partial t} = -\frac{\theta}{\tau} + \psi\left[1 + \cos 2\omega t\right] \tag{8}$$

Where $$\tau = \frac{mc}{h_c A} \text{ and } \psi = \frac{I_0^{\,2} R}{2mc} \tag{9}$$

Thus the heat generation term in equation (8) has two components:

(i) a DC component = ψ, (ii) an AC component = $\psi \cos 2\omega t$. Since this is a linear equation in θ, we can write $\theta = T_{DC} + T_{AC}$. Note that T_{DC} is the DC temperature rise due to an AC current. For T_{DC} the governing equation is,

$$0 = \frac{-T_{DC}}{\tau} + \psi \Rightarrow T_{DC} = \tau\psi = \frac{I_0^{\,2} R}{2h_c A} \tag{10}$$

The governing equation for T_{AC} is,

$$\frac{\partial T_{AC}}{\partial t} = -\frac{T_{AC}}{\tau} + \psi \cos 2\omega t \tag{11}$$

Now let $T_{AC} = B\cos 2\omega t + C\sin 2\omega t$. Substituting in equation (11) we can show that

$$B = \frac{\psi\tau}{\left[1 + (2\omega\tau)^2\right]} \text{ and } C = \frac{\psi 2\omega\tau^2}{\left[1 + (2\omega\tau)^2\right]}$$

Thus T_{AC} can be written as,

$$T_{AC} = \frac{\psi\tau}{\left[1 + (2\omega\tau)^2\right]} \cos 2\omega t + \frac{\psi 2\omega\tau^2}{\left[1 + (2\omega\tau)^2\right]} \sin 2\omega t \tag{12}$$

Now the amplitude or the maximum value of T_{AC} is given by,

$$\left|T_{AC}\right| = \frac{\psi\tau}{\left[1 + (2\omega\tau)^2\right]} \sqrt{1 + (2\omega\tau)^2} \tag{13}$$

From equation (9) and (10) we see that $T_{DC} = \psi\tau$.

Hence, the peak AC and DC temperature rises can be related as

$$T_{AC} = T_{DC} \Big/ \sqrt{1 + (4\pi f\tau)^2} \tag{14}$$

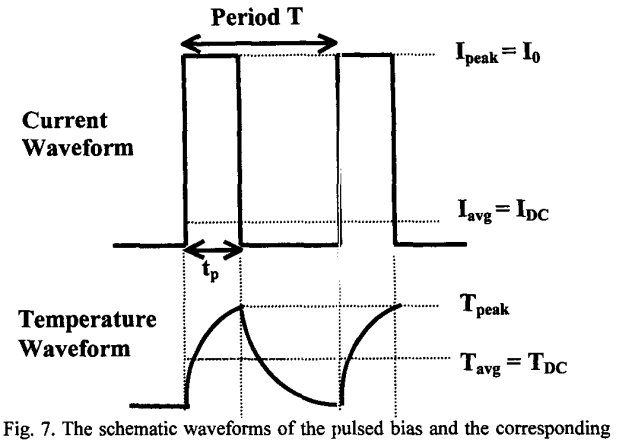

Fig. 7. The schematic waveforms of the pulsed bias and the corresponding temperature rise.

Where $\omega = 2\pi f$. Figure 4 plots experimental data indicating this behavior and yields a time constant $\tau = 26$ μs. The experiments were performed in vacuum in order to get rid of the effect on the deflection of the cantilever due to the heating by the surrounding gas [14]. Since the internal time constant of the W-plug via, $\tau_{via} = d^2/\alpha_W$ (here d is the via diameter, and α_W is the thermal diffusivity of W), is of the order of 1 ns, the observation of $\tau = 26$ μs suggests that the surrounding materials, composed mainly of oxide and nitride, must be involved in heat spreading. Using this first-order analysis, T_{DC} was found as a function of sinusoidal current stress and plotted in Fig. 5, where the $T_{DC} \propto I^2$ behavior can be seen.

We also measured the self-heating of the W-via under a DC current stress using the temperature dependence of the resistivity of the W-plug as shown in Fig. 6. For this, the temperature coefficient of resistance (TCR) of the W-plug was experimentally determined to be ~1.01 × 10^{-3} K^{-1} from Kelvin measurements. We can observe from Fig. 6 that a DC current of (say 10 mA) results in a temperature rise of about 25 °C. The corresponding peak current for the sinusoidal bias is 14.14 mA, which gives a DC temperature rise (from Fig. 5) of around 20 °C, which is lower than the temperature rise under DC current stress. This is expected since the DC temperature rise under sinusoidal bias is estimated from the measured AC temperature rise using SJEM experiment, where heat diffusion into the dielectric surrounding the via, and into the metal at the top and bottom of the via, results in a slightly lower measured temperature.

Self-Heating Analysis under Pulsed Bias

To study the thermal behavior of the W-via under a pulsed bias, experiments were conducted at $f = 25$ KHz, pulse amplitude of 2 V, and pulse widths, t_p, from 50 ns to 500 ns. The schematic representation of the pulsed current and the corresponding temperature rise is shown in Fig. 7.

The current amplitude for the pulsed bias can be expressed as,

$$I = \begin{cases} I_0, & for \;\; nT < t < nT + t_p \\ 0, & for \;\; nT + t_p < t < (n+1)T \end{cases} \tag{15}$$

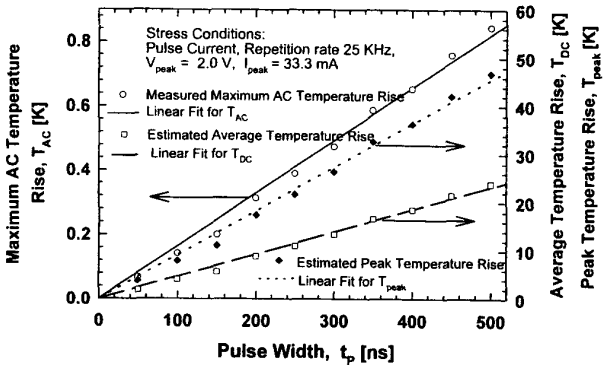

Fig. 8. The first harmonic, average and peak temperature rise as a function of the pulsed width of applied pulsed current. The stress condition corresponds to a current density of 2.65×10^7 A/cm^2 in the via and 3.47×10^6 A/cm^2 in the metal line.

where n is some integer, t_p is the on time of the pulses and T is the time period. The governing heat equation can be written as,

$$\frac{\partial \theta}{\partial t} = -\frac{\theta}{\tau} + \frac{I^2 R}{mc} \tag{16}$$

Here τ is the characteristic time constant of the first order equation. The Fourier analysis of the temperature rise yields,

$$\theta = \theta_0 + \sum_{n=1}^{\infty} \theta_n e^{in\omega t} \tag{17}$$

Where $$\theta_n = \frac{1}{T}\int_0^T \theta e^{-in\omega t} dt \tag{18}$$

And $$\theta_0 = \frac{1}{T}\int_0^T \theta dt \tag{19}$$

The first harmonic (25 KHz) of the via temperature rise, θ_1, can be calculated from equation (18) by multiplying equation (16) with $e^{-i\omega t}$ and integrating each term from 0 to T. This yields

$$\theta_1 = \frac{1}{T}\int_0^T \theta e^{-i\omega t} dt = \frac{I_0^2 R}{mcT} \frac{(1 - e^{-i\omega t_p})}{i\omega(i\omega + \frac{1}{\tau})} \tag{20}$$

For $t_p << T$, $1 - e^{-i\omega t_p} \approx i\omega t_p$ and thus θ_1 is given by,

$$\theta_1 = \frac{I_0^2 R}{mcT} \frac{t_p}{(i\omega + \frac{1}{\tau})} \tag{21}$$

and thus the amplitude of θ_1 is given by,

$$|\theta_1| = \sqrt{\theta_1 \bar{\theta}_1} = \frac{I_0^2 R t_p}{mcT} \frac{1}{\sqrt{\omega^2 + \frac{1}{\tau^2}}} \tag{22}$$

Similarly, the average temperature rise θ_0 can be calculated from equation (19) by simply integrating equation (16) from 0 to T. This yields,

$$\theta_0 = \frac{1}{T}\int_0^T \theta dt = \frac{I_0^2 R t_p}{mcT} \tau \tag{23}$$

In our experiments $T_{AC} = \theta_1$ was measured by measuring the amplitude of the first harmonics of the expansion signal. Figure 8 shows that T_{AC} varies linearly with pulse widths, in accordance with equation (22). Here I_0 is the peak current, R is the via electrical resistance, and (mc) is the thermal capacity of W-via. The average temperature $T_{avg} = T_{DC} = \theta_0$ can be estimated by this analysis from the ratio of equation (22) to equation (23) which gives,

$$\frac{T_{AC}}{T_{DC}} = \frac{1}{\sqrt{1 + (2\pi f \tau)^2}} \tag{24}$$

Similarly one can obtain the peak temperature rise, T_{peak} in the following way. The heat equation during the "on" and "off" times during the pulsed stress can be written as,

$$\frac{\partial \theta_{on}}{\partial t} = -\frac{\theta_{on}}{\tau} + \frac{I_0^2 R}{mc} \quad \text{for } nT < t < nT + t_p \tag{25}$$

and $$\frac{\partial \theta_{off}}{\partial t} = -\frac{\theta_{off}}{\tau} \quad \text{for } nT + t_p < t < (n+1)T \tag{26}$$

The solution to equation (25) is given by,

$$\theta_{on} = C_1 \exp(-\frac{t}{\tau}) + \frac{I_0^2 R \tau}{mc} \tag{27}$$

Similarly, the solution to equation (26) is given by,

$$\theta_{off} = C_2 \exp(-\frac{t}{\tau}) \tag{28}$$

We can get C_1 and C_2 by applying the following two boundary conditions to equation (27) and equation (28).

(i) Steady periodic behavior: $\theta_{on}(nT) = \theta_{on}((n+1)T)$ and,

(ii) Temperature Continuity: $\theta_{on}(nT + t_p) = \theta_{off}(nT + t_p)$

and therefore we get T_{peak} from the fact that

$$T_{peak} = \theta_{on}(nT + t_p) = \theta_{off}(nT + t_p)$$

This yields,

$$T_{peak} = \frac{I_0^2 R \tau}{mc} \left[\frac{1 - \exp(-\frac{t_p}{\tau})}{1 - \exp(-\frac{T}{\tau})} \right] \tag{29}$$

Therefore, the peak temperature rise T_{peak} can be estimated by this analysis from the ratio of equation (23) to equation (29) supposing $t_p << \tau$, which gives,

$$\frac{T_{DC}}{T_{peak}} = (f\tau)[1 - \exp(-1/f\tau)] \tag{30}$$

These values are also shown in Fig. 8.

CONCLUSIONS

In conclusion, this paper demonstrates that SJEM can be used to measure the spatial temperature distribution in VLSI interconnect leads and vias and to study their steady state and dynamic thermal behavior under sinusoidal and pulsed current stress. The extracted temperature contour map gives quantitative information on the spatial distribution of temperature surrounding a small geometry via and the location of the hot-spot. The spatial distribution of temperature rise could also be useful in modeling

via electromigration and other thermally induced via failure mechanisms, which are strongly influenced by temperature gradients around the via. The thermal time constant of the via structure has also been determined from the measured AC frequency dependence of the temperature rise. Furthermore, the average (DC) and peak temperature rise under pulsed stress condition have been estimated from the measured first harmonic temperature rise. Thus, the sub-100 nm resolution of SJEM can be potentially employed to design thermally robust multilevel interconnect structures, and improve reliability. It can be used to investigate current crowding effects and can help determine the impact of different via and lead designs on the thermal characteristics of multi-level deep submicron interconnect structures.

ACKNOWLEDGMENTS

This work was in part, supported through the National Science Foundation through Grant CTS-9796166, Texas Instruments Inc., and the MICRO program. The authors would also like to thank Professor Andrea Scorzoni of Institute of Electronics, University of Perugia, Italy, for reviewing this paper. KB would also like to thank Dr. William Hunter of Texas Instruments Inc., for some helpful discussions.

REFERENCES

[1] T. Kwok, T. Nguyen, P. Ho, and S. Yip, "Current density and temperature distributions in multilevel interconnections with studs and vias," *Proc. IEEE Int. Reliab. Phys. Symp,* 1987, pp. 130-135.

[2] K. Weide, and W. Hasse, "3-Dimensional simulations of temperature and current density distribution in a via structure," *Proc. IEEE Int. Reliab. Phys. Symp,* 1992, pp. 361-365.

[3] J. T. Trattles, A. G. O'Neill, and B. C. Mecrow, "Three dimensional finite element investigation of current crowding and peak temperatures in VLSI multilevel interconnections," *IEEE Trans. Electron Devices*, vol. 40, pp. 1344-1347, 1993.

[4] K. Banerjee, A. Amerasekera, G. Dixit, N. Cheung and C. Hu, "Characterization of contact and via failure under short duration high pulsed current stress," *Proc IEEE Int. Reliab. Phys. Symp,* 1997, pp. 216-220.

[5] K. Banerjee, A. Amerasekera, N. Cheung and C. Hu, "High-current failure model for VLSI interconnects under short-pulse stress conditions," *IEEE Electron Device Letters,* vol. 18, No. 9, pp. 405-407, 1997.

[6] Y. S. Ju, and K. E. Goodson, "Thermal mapping of interconnects subjected to brief electrical stresses", *IEEE Electron Device Letters,* vol. 18, pp. 512-514, 1997.

[7] S. Kondo, and K. Hinode, "High-resolution temperature measurement of void dynamics induced by electromigration in aluminum metallization," *Appl. Phys. Lett.*, vol. 67, pp. 1606-1608, 1995.

[8] J. Hiatt, "A method of detecting hot spots on semi-conductors using liquid crystals", *Proc IEEE Int. Reliab. Phys. Symp,* 1981, pp. 130-133.

[9] K. E. Goodson, and M. Asheghi, "Near-field optical thermometry," *Microscale Thermophysics Engineering*, Vol. 1, 1997, pp. 225-235.

[10] J. Varesi, and A. Majumdar, "Scanning Joule expansion microscopy at nanometer scales," *Appl. Phys. Lett.*, vol. 72, pp. 37-39, 1998.

[11] A. Majumdar, and J. Varesi, "Nanoscale temperature distributions measured by scanning Joule expansion microscopy," *ASME J. Heat Transfer*, vol. 120, pp. 297-305, 1998.

[12] H. S. Carslaw, and J. C. Jaeger, *Conduction of Heat in Solids*, pp. 66, Clarendon Press, Oxford, 1959.

[13] A. F. Mills, "*Heat and Mass Transfer*," IRWIN Inc., 1995, Chapter 1, pp. 30-34.

[14] K. Luo, Z. Shi, J. Varesi, and A. Majumdar, "Sensor nanofabrication, performance, and conduction mechanisms in scanning thermal microscopy," *Journal of Vacuum Science and Technology B*, Vol. 15, pp 349-360, 1997.